Hindawi Publishing Corporation
Journal of Sensors
Volume 2014, Article ID 150549, 4 pages
http://dx.doi.org/10.1155/2014/150549

Research Article

A Novel Subnanosecond Monocycle Pulse Generator for UWB Radar Applications

Xinfan Xia,[1,2] Lihua Liu,[1] Shengbo Ye,[1,2] Hongfei Guan,[1] and Guangyou Fang[3]

[1] *Key Laboratory of Electromagnetic Radiation and Sensing Technology, Chinese Academy of Sciences, No. 19, North 4th Ring Road West, Haidian District, Beijing 100190, China*
[2] *University of Chinese Academy of Sciences, No. 19A Yuquan Road, Beijing 100049, China*
[3] *Chinese Academy of Sciences, 52 Sanlihe Road, Beijing 100864, China*

Correspondence should be addressed to Xinfan Xia; cindyxia00@126.com

Received 24 July 2014; Revised 26 September 2014; Accepted 7 October 2014; Published 15 December 2014

Academic Editor: Aaron T. Ohta

A novel ultra-wideband (UWB) monocycle pulse generator with good performance is designed and demonstrated in this paper. It contains a power supply circuit, a pulse drive circuit, a unique pulse forming circuit, and a novel monopolar-to-monocycle pulse transition circuit. The drive circuit employs wideband bipolar junction transistors (BJTs) and linear power amplifier transistor to produce a high amplitude drive pulse, and the pulse forming circuit uses the transition characteristics of step recovery diode (SRD) effectively to produce a negative narrow pulse. At last, the monocycle pulse forming circuit utilizes a novel inductance L short-circuited stub to generate the monocycle pulse directly. Measurement results show that the waveform of the generated monocycle pulses is over 76 V in peak-to-peak amplitude and 3.2 ns in pulse full-width. These characteristics of the monocycle pulse are advantageous for obtaining long detection range and high resolution, when it is applied to ultra-wideband radar applications.

1. Introduction

Ultra-wideband (UWB) technology has received significant interests for a lot of applications, for example, nondestructive evaluation (NDE) of highway structures [1], geophysical prospecting, short-range in-building communications [2], vital sign detection [3], and so on. In these ultra-wideband communication and radar applications, step, Gaussian, and monocycle pulses are very important. And pulse generators of fixed pulse durations are used. These pulse types have a common characteristic of extremely wide instantaneous bandwidth and can be transmitted without carrier. Among them, the spectrum of the monocycle pulse contains very little low frequency and no DC components. It facilitates the design of other system components such as antennas, amplifiers, and receivers. What is more, this pulse type matches well with the transmitting antenna and owns better signal characteristics that can reduce distortion for the transmitting and receiving signals [4].

Several methods are used to produce monocycle pulses: one is using transmission line pulse forming networks or short-circuited stubs [5] and another is using RC or LC differentiators [6] to generate monocycle pulse. However, these methods usually used behind a SRD sharpener will introduce pulse distortion and much ringing into the output waveform. Therefore, how to reduce ringing behind the monocycle pulse is the key problem.

In this paper, a novel UWB monocycle pulse generator is showed. It contains power supply circuit, drive circuit, SRD pulse forming circuit, and monocycle pulse forming circuit. The drive circuit uses bipolar junction transistor to speed up the trigger signal and uses wideband linear power amplifier transistor to produce drive pulse with high amplitude. SRD pulse forming circuit uses two SRDs connected in series with a pulse-shaping network, which employs a Schottky diode. Monocycle pulse forming circuit consists of an inductance L short-circuited stub and an additional ringing suppression circuit, which combines two Gaussian pulses with opposite phase to form a monocycle pulse and reduce the ringing level of the output waveform effectively. The structure diagram of this novel generator is shown in Figure 1. The output monocycle pulse is over 76 V in peak-to-peak amplitude and

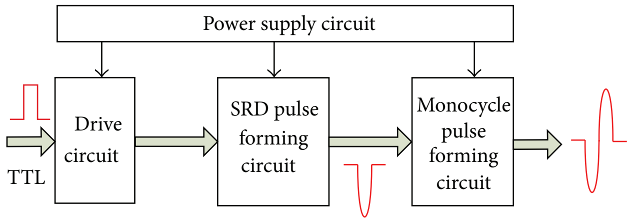

Figure 1: Structure diagram of the discussed monocycle pulse generator.

3.2 ns in pulse width. The ringing level is below 1.5%. These good performances make the UWB radar system obtain high resolution and long detection range for penetrating applications.

2. Power Supply Circuit

This monocycle pulse generator needs two kinds of power supply voltage. They are produced by the power supply circuit. The specific circuit diagram is shown in Figure 2. The implemented step-up voltage regulator $U1$ of type LM2577-ADJ is manufactured by National Semiconductor. The type of fast recovery diode $D5$ is MR851, which is manufactured by ON Semiconductor. The output voltage V_{CC2} is 56 V, while the input voltage V_{in} is 15 V ($R8 = 100\,k\Omega$, $R9 = 1\,k\Omega$). The implemented positive voltage regulator $U2$ of type ZR78L12 is manufactured by Zetex Semiconductors. It can change 15 V into +12 V as V_{CC1}.

3. Drive Circuit

This design consists of two bipolar junction transistors Q1 (BFG35) and Q2 (BFG31), a wideband linear power amplifier transistor Q3, and energy storage capacitors. The type of Q3 is B3-28, which is manufactured by ASI Semiconductor. Drive circuit uses the switching characteristic of Q1 and Q2 to shaping the trigger signal step by step. Then, it uses the power transistor Q3 with stronger driving ability to produce the drive pulse with high amplitude and short pulse duration, which is hardly produced by normal RF transistor and microwave transistor. The specific circuit diagram is shown in Figure 3. It can offer a negative drive pulse to the input of the SRD pulse forming circuit.

4. SRD Pulse Forming Circuit

SRD is a kind of switching device which uses the charge-storage effect of minority carriers. There is steep impurity distribution area in its PN junction boundaries. It is the key component in the SRD pulse forming circuit. Transition time and minority carrier lifetime are the most important parameters of SRD. The transition time determines the minimum achievable pulse transition time, which is directly relevant to the rising time or falling time of output pulses. Minority carrier lifetime directly decides the peak amplitude of the output pulses by affecting the charge storage time under reverse-bias conditions. This design chooses appropriate

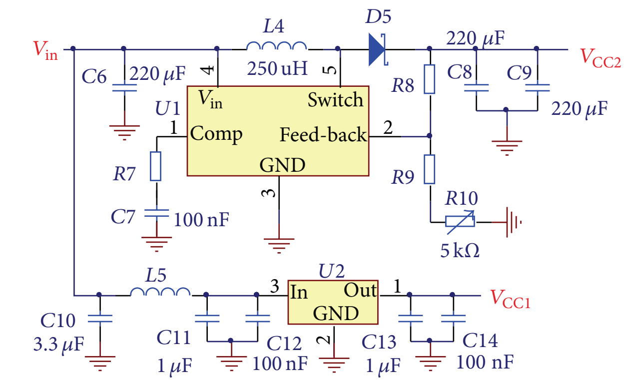

Figure 2: Power supply circuit.

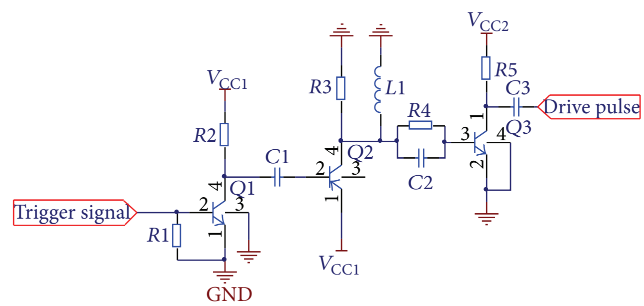

Figure 3: Circuit diagram of drive circuit.

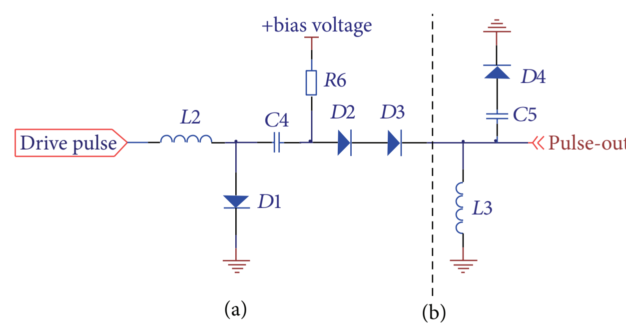

Figure 4: The schematic of SRD pulse forming circuit and monocycle pulse forming circuit. (a) SRD pulse forming circuit, (b) monocycle pulse forming circuit.

SRDs $D2$ and $D3$ connected in series to achieve a Gaussian pulse with maximum achievable amplitude and suitable pulse width. The MP4062 SRD in the P2 package [7] and BAT62-03W Schottky Diode (SD) in the SOD-323 package [8] are used in the SRD pulse forming circuit. The specific circuit diagram of the SRD pulse forming circuit is shown in part (a) of Figure 4. When the negative drive pulse does not come, the SRDs and Schottky Diode $D1$ are forward biased by +bias voltage and V_{CC2}, respectively. The minority carriers are stored near the PN junction of SRDs. When the negative drive pulse arrives, SD is reverse bias and cuts off immediately. It does not influence the circuit at the moment. The movement of the minority carriers forms reverse current by the reverse electric field effect. When the minority carriers are extracted completely, the reverse current quickly fell to minimum value, and the SRD turns off in a very short time. Thus a reverse current step is produced and a negative narrow pulse is generated at the cathode of $D3$. $L2$ is used to store energy. $D1$ is used to reduce the overshoot of the narrow pulse and also cut down the reflected wave formed by the poststage circuit.

5. Monocycle Pulse Forming Circuit

This design uses inductance $L3$ as a short-circuited microstrip line. The specific circuit diagram of the monocycle pulse forming circuit is shown in part (b) of Figure 4. The negative narrow pulse at the cathode of $D3$ propagates in two directions away from SRDs. One is to the output port and the other is to the short-circuited inductance $L3$. The latter is reflected back with inverted polarity as echoingcharacteristics of the short-circuited transmission line and then propagates to the output with time delay. Finally, a monocycle pulse is formed by the synthesis of the delayed inverted narrow pulse and the pulse propagating unchanged from the SRDs to the output port. An additional ringing suppression circuit is placed at the end of the design. It consists of capacitance $C5$ and diode $D4$. It reduces the trailing of the monocycle pulse effectively. The 1N4148 in the SOD27 package are used for $D4$.

6. Measurement Result

The monocycle pulse generator is fabricated on FR4 glass epoxy substrate. The relative dielectric constant of the substrate is 4.5 and the thickness is 1.6 mm. A photograph of the generator is shown in Figure 5. The circuit is simple, and it is attractive for practical application.

7. Measurement Result

A TTL signal with a repetition frequency from 100 kHz to 10 MHz is used as trigger signal. The output voltage of the monocycle pulse generator has been measured choosing the following element values: $C1 = 100$ pF, $C2 = 10$ pF, $C3 = 1$ nF, $C4 = 10$ nF, $5 = 10$ nF, $R1 = 50\,\Omega$, $R2 = R3 = 200\,\Omega$, $R5 = 1\,\text{k}\Omega$, and $L2 = 10$ uH. The output monocycle pulses measured by a wideband oscilloscope are showed in Figure 6. The trailing behind the main pulse is extremely small. The peak-to-peak amplitude ($V_{\text{p-p}}$), the rise time of the peak-to-peak amplitude (t_r), pulse full-width (τ_p), and the ringing level at 1 MHz and 3 MHz PRF are summarized in Table 1. The normalized power spectrum of the output monocycle pulse calculated using the Fourier transform with Matlab is shown in Figure 7. The 20 dB bandwidth is 1.25 GHz. And the output monocycle pulses at different PRF are shown in Figure 8. It shows that the influence of the PRF on the shape of the output waveforms is negligible. This monocycle pulse generator can work well up to 10 MHz.

8. Conclusion

This monocycle pulse generator contains a power supply circuit, a drive circuit, a SRD pulse forming circuit, and a monocycle pulse forming circuit. The key technology of this pulse generator is drive circuit and the monocycle pulse forming method. The drive circuit connects BJTs and wideband linear power amplifier transistor together to produce drive pulse with high amplitude. The monocycle pulse forming circuit makes inductance L equivalent be a short-circuited microstrip line and utilizes the reflection characteristics of

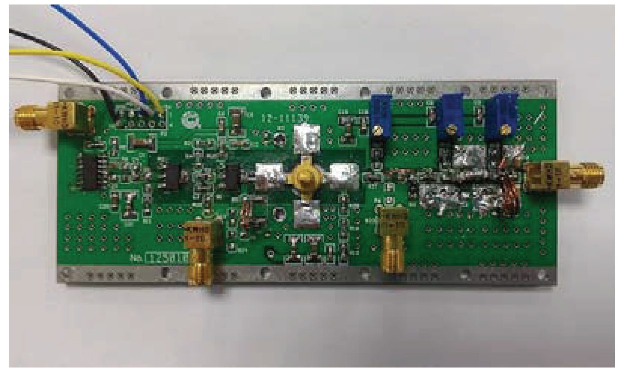

Figure 5: The photograph of the monocycle pulse generator.

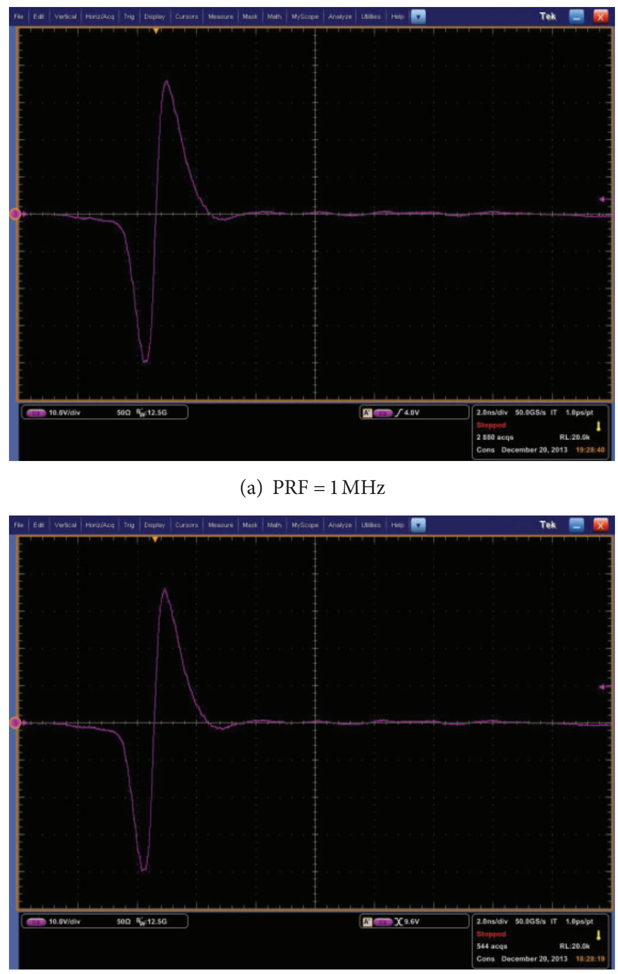

(a) PRF = 1 MHz

(b) PRF = 3 MHz

Figure 6: The output pulse waveforms of the monocycle pulse generator at different PRF.

TABLE 1: Monocycle pulse parameters.

PRF	$V_{p\text{-}p}$ (V)	t_r (ps)	Full-width τ_p (ns)	Ringing level (%)
1 MHz	76.0	700	3.2	1.48
3 MHz	75.8	700	3.2	1.48

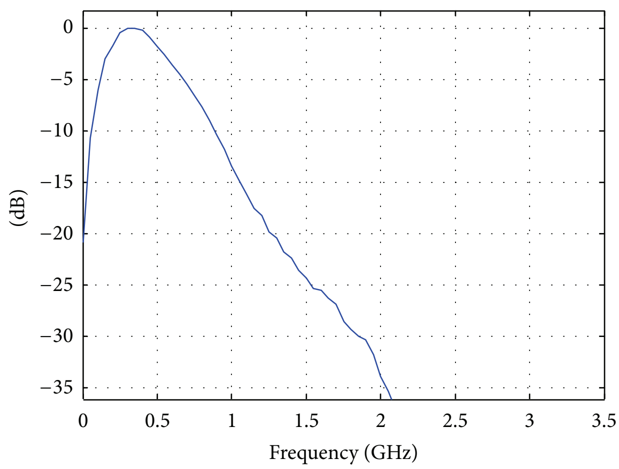

FIGURE 7: Calculated power spectrum of the output pulses normalized to the peak value.

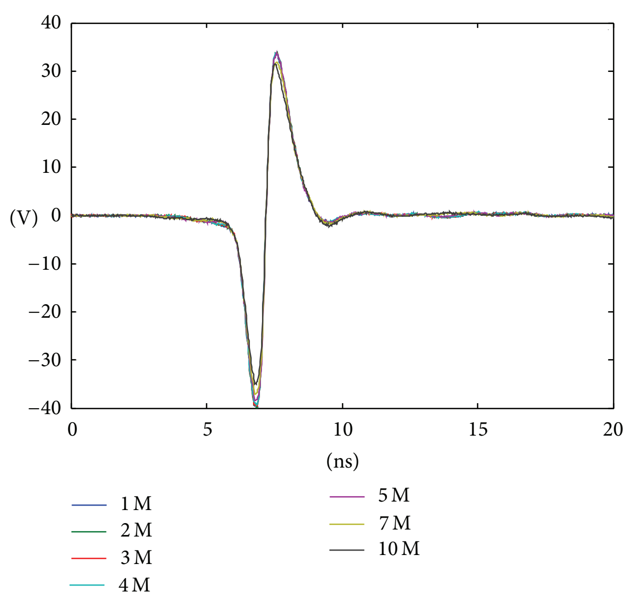

FIGURE 8: The output pulse waveform of the monocycle pulse generator at different PRF.

the short-circuited transmission line to synthesis of a monocycle pulse. Moreover, an additional circuit consists of a capacitance and a diode connected in series to reduce the ringing level. As the measurement results showed, this monocycle pulse generator produces a monocycle pulse with good symmetry and low ringing level below 1.5%. Its peak-to-peak amplitude is 76 V, and its pulse full-width is approximately 3.2 ns. Therefore, this design can be used well for UWB radar application such as vital sign detection, penetrating thick and lossy building walls or ground with high resolution and good detection range.

Conflict of Interests

The authors declare that there is no conflict of interests regarding the publication of this paper.

Acknowledgment

This work was supported by the National High Technology Research and Development Program of China (863 Program) under Grants 2012AA061403 and 2012AA121901.

References

[1] J. Hugenschmidt and P. Fürholz, "ATRAS—an automated GPR system for data acquisition and storage for roads and bridges," in *Proceedings of the 14th International Conference on Ground Penetrating Radar (GPR '12)*, pp. 448–453, Shanghai, China, June 2012.

[2] N. Riaz and M. Ghavami, "Analytical performance evaluation of ultra-wideband multiple access schemes for different wireless sensor network application environments," *IET Communications*, vol. 3, no. 9, pp. 1473–1487, 2009.

[3] J. Li, L. Liu, Z. Zeng, and F. Liu, "Advanced signal processing for vital sign extraction with applications in UWB radar detection of trapped victims in complex environments," *IEEE Journal of Selected Topics in Applied Earth Observations and Remote Sensing*, vol. 99, pp. 1–9, 2013.

[4] T. Xia Sr., A. S. Venkatachalam, and D. Huston, "A high-performance low-ringing ultrawideband monocycle pulse generator," *IEEE Transactions on Instrumentation and Measurement*, vol. 61, no. 1, pp. 261–266, 2012.

[5] P. W. Smith, *Transient Electronics: Pulsed Circuit Technology*, John Wiley & Sons, New York, NY, USA, 2002.

[6] J. H. Reed, *An Introduction to Ultra Wideband Communication Systems*, Prentice Hall PTR, 2005.

[7] MP40 Step Recovery Diodes, "M-Pulse Microwave," http://www.mpulsemw.com/SRD_Diode.htm.

[8] BAT 62-03W Schottky Diode, http://www.infineon.com/cms/en/search.html#!term=bat62series&view=all.

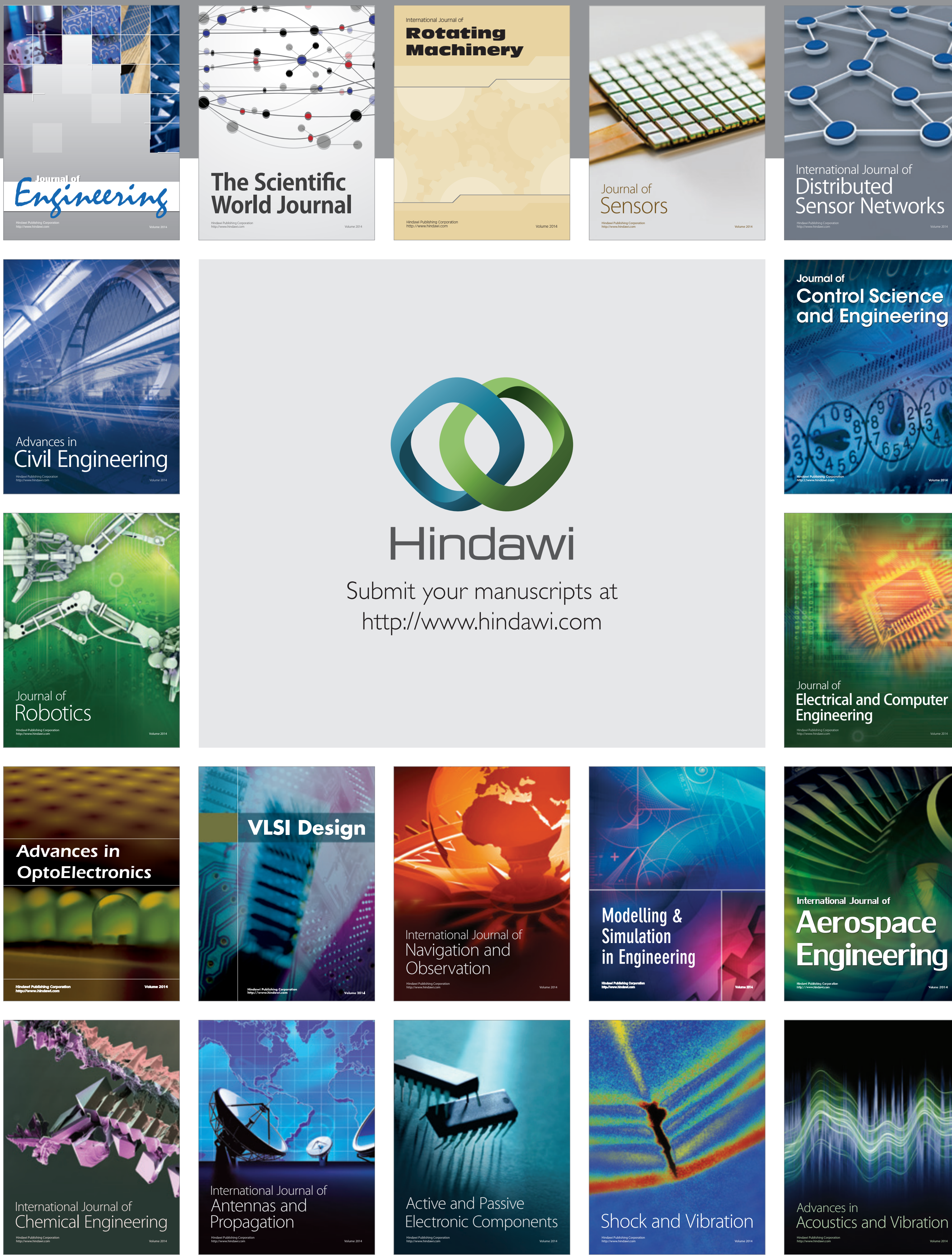
Journal of Engineering
The Scientific World Journal
International Journal of Rotating Machinery
Journal of Sensors
International Journal of Distributed Sensor Networks
Advances in Civil Engineering
Hindawi
Submit your manuscripts at http://www.hindawi.com
Journal of Control Science and Engineering
Journal of Robotics
Journal of Electrical and Computer Engineering
Advances in OptoElectronics
VLSI Design
International Journal of Navigation and Observation
Modelling & Simulation in Engineering
International Journal of Aerospace Engineering
International Journal of Chemical Engineering
International Journal of Antennas and Propagation
Active and Passive Electronic Components
Shock and Vibration
Advances in Acoustics and Vibration